Welding in the World
https://doi.org/10.1007/s40194-024-01859-6

RESEARCH PAPER

Fatigue performance of repair-welded and HFMI-treated transverse stiffeners

J. Schubnell[1] · M. Burdack[1] · N. Hiltscher[2] · P. Weidner[2] · T. Ummenhofer[2] · M. Farajian[3]

Received: 18 July 2024 / Accepted: 18 October 2024

Abstract

Large portions of infrastructure buildings, for example, highway and railway bridges, are steel constructions and reach the end of their service life due to an increase of traffic volume. Repair welding can restore the current welded constructional detail with a similar fatigue strength. However, due to the increase of fatigue loading (traffic), an increase of fatigue strength is needed in such bridge structures. For this reason, the combination of repair welding and high-frequency mechanical impact (HFMI) treatment was investigated in this study in order to quantify the increase of fatigue life by combining both methods. For this, transverse stiffeners made of steel grade S355J2 + N were subjected to fatigue loading until a pre-determined crack depth was reached. The cracks were detected by non-destructive testing methods. Weld repair was realized by removing the material containing the crack and re-welded by a gas metal arc welding (GMAW) process, following that post weld treated was applied by HFMI-treatment and the specimens were subjected to fatigue loading again. Hardness profiles, weld geometries, and residual stress states were investigated for both the original and the repaired condition. In the repaired condition without additional HFMI treatment, a similar fatigue life than in the original condition is observed for the specimens. The repair-welded and HFMI-treated specimens reach a significant higher fatigue life compared to the repaired ones in the as-welded condition.

Keywords Fatigue · Welded joints · Repair welding · Post weld treatment · High-frequency mechanical impact · HFMI · Residual stress · Transverse stiffener

Recommended for publication by Commission XIII - Fatigue of Welded Components and Structures

✉ J. Schubnell
jan.schubnell@iwm.fraunhofer.de

M. Burdack
michael.burdack@iwm.fraunhofer.de

N. Hiltscher
nicolas.hiltscher@kit.edu

P. Weidner
philipp.weidner@kit.edu

T. Ummenhofer
thomas.ummenhofer@kit.edu

M. Farajian
farajian@slv-duisburg.de

[1] Fraunhofer Institute for Mechanics of Materials, Freiburg, Germany

[2] KIT Steel & Lightweight Structures, Karlsruhe Institute of Technology (KIT), Karlsruhe, Germany

[3] GSI Gesellschaft Für Schweißtechnik International mbH, Duisburg, Germany

1 Introduction

Retrofitting of steel constructions in infrastructure buildings like bridges and offshore structures has gained more and more importance in recent years. Especially railway or highway bridges are exposed to a strongly increasing rail cargo and traffic volume. This leads to an increasing load spectrum of such structures and, thus, to an increasing fatigue damage. In many cases, welded constructional details are especially affected as a reason of their comparably low fatigue resistance. In the Federal Republic of Germany, nearly 50% of the steel bridges are built before the year 1980 [1], and around 55% of the railway bridges are built before the year 1950 [2]. Similar conditions are reported from the USA where around 85% of the bridges in Minnesota were built before the year 1986 [3]. Originally, these structures were designed for significant lower traffic loads and a significant higher number of repair cases are expected for the future [4].

The right choice of the respective repair strategy is an important factor to extend the fatigue life of steel structures

Published online: 31 October 2024

containing cracks [3]. Usually, fatigue cracks are detected by visual inspection or non-destructive testing methods in periodic time intervals. After the detection of a crack, possible repair methods are the usage of bolted splices or by grinding and re-welding the material [5]. However, bolted splices are not always efficient for relatively minor fatigue damage cases especially if the available working space around the damaged area is limited [6]. Compared to the conventional bolt splice method, repair welding is a more cost-efficient solution and can be performed with less time effort. However, possible weld defects like splatters, undercuts or cold laps can be induced by the re-welding process and might only lead to a comparatively small extended lifespan after the retrofitting measure.

Former studies [5, 7–19] have shown that the fatigue strength of the original welded detail can be restored by repair welding without any further post weld treatment. However, regarding the aforementioned increase of fatigue loading or load cycles by increasing traffic, a simple restoration of the original weld detail would lead to multiple repairs in the future again. Only in a minor number of repair cases (ca. 8%) in bridges an insufficient weld quality of the original detail was the reason [4] for the respective measure. In 78% of the reported cases, an impropriate structural detail or an underestimation of the loading condition is the reason for repair measures of bridge structures. This means, a restoration of the original weld detail while reaching a similar fatigue strength would lead to similar repairs in the future. Thus, only a significant increase of fatigue strength of welded structures could prevent from extensive and costly repair measures in future. Regarding the significant amount of bridge structures which are already in a critical state, this aspect gains more and more economical importance.

Referring to this, possibilities for increasing the fatigue strength of welded structures by retrofitting actions are of major importance. Due to numerous different weld-details which are found in steel bridges and constructions [4, 5, 20, 21], perhaps no universal solution exits. According to documented repair cases of Yokoyama and Miki [4] as well as the IIW-document XIII-2284r1-09 [5], in many cases, a change of the structural design was used (for example, the application of cover plates or additional stiffeners). However, these approaches are costly and time consuming. In some cases, fatigue cracks again started at the additional applied stiffeners or cover plates [5]. For these reasons, an efficient use of post weld treatment methods might be a solution to increase the fatigue strength of repair-welded joints without large efforts.

High-frequency mechanical impact (HFMI) treatment is a mechanical surface treatment process that was investigated and used for post weld treatment of welded joints since the late 1990s. The beneficial effect of fatigue life improvement by HFMI is statistically proved and described by several international [22] and national standards [23] depending on the respective welded detail, the basic material yield strength, the stress ratio R, and the plate thickness. Several studies have been focused on retrofitting of preloaded welded joints by HFMI-treatment [24–33]. These studies have shown that a significant fatigue life extension according to the current recommendations [22, 23] could be reached. Further investigations show that HFMI treatment still leads to a fatigue life extension for welded joints containing cracks with a depth in the range of 0.5 to 4 mm [29, 31, 33–35]. However, currently, there are very few investigations regarding the combination of repair welding and HFMI-treatment available.

The aim of this work was to quantify the fatigue strength of repair-welded and HFMI-treated transverse stiffeners. For repair welding, the approach by Ladendorf et al. [1] and Schubnell et al. [10] was used. A stepwise procedure containing the fatigue test in original condition, crack detection by NDT-methods, grinding, multi pass repair-welding including HFMI as a post weld treatment, and the conduction of fatigue tests in the retrofitted condition was performed.

2 Material and specimen details

The commonly used mild structural steel S355J2 + N in normalized condition with a yield strength of 415 MPa was used. The chemical compositions of the base materials are shown in Table 1, and the mechanical properties are given in Table 2. The chemical composition was measured by spectral analysis or taken from data sheets of the filler metal. In general, the base material, the welded constructional detail and the welding parameters are identical compared to previous studies [1, 10].

Table 1 Chemical composition of the investigated base materials

Materials	Elements (wt%) (Fe = bal.)													
	C	Mn	Si	P	S	Cr	Ni	Mo	V	W	Cu	Al	Ti	CEV*
S355J2 + N	0.161	1.47	0.17	0.0107	0.0053	0.040	0.035	0.007	0.008	0.004	0.015	0.032	0.0125	0.42
G4Si1**	0.08	1.65	1.0											

*According to DIN EN 10025–2 [36]; **Data sheet

Table 2 Mechanical properties of the investigated base materials

Materials	Yield strength [MPa]	Ultimate strength [MPa]	Elongation [%]	Hardness [HV10]	Generic name
S355J2 + N	415	565	25*	169	-
G4Si1**	390–490	510–610	≥ 25		SG3

*Data sheet

In this work, the investigated fillet welds were manufactured by a gas metal arc welding (GMAW) process. The weld detail was a double-sided transverse stiffener. The dimensions of the specimens are shown in Fig. 1a, and the cross section of the actual welds are shown in the macro sections in Fig. 1b. G4Si1 with a wire diameter of 1.2 mm was used as a filler material for the welding process of the specimens out of S355J2 + N according to DIN EN 757:1997–95. The inert shielding gas M21-ArC-18 was used with a flow rate of 15–18 l/min. The welding parameters for all cases are given in Table 3. For each material, the same welding parameters for each weld were used. For all welds, the quality class B according to ISO 5817:2023 [37] was reached.

3 Repair procedure and post weld treatment

As a repair or retrofitting procedure, the approach of former studies was used [1, 10] based on the approach of the Federal Highway Administration of the United States, derived by a workshop of experts under the supervision of Dexter and Ocel [3], illustrated in Fig. 2. The repair procedure by welding in this study uses the following steps: at first, the crack detection is necessary by visual testing (VT). After that, magnetic particle testing (MT) is used to determine the specific length and orientation of the crack. After detection, the removal of the crack is performed by manual grinding. Between the removal steps, MT is applied in order to follow the crack path and to obtain the information of the actual crack depth. In case the crack depth is below one-half of the plate thickness, a one-sided repair was made (step 1 to 4, illustrated in Fig. 2a). If the crack was not completely removed after reaching a depth of 0.5 times the sheet thickness t, the material removal should be made to a depth of three-quarter of the plate thickness, and the repair procedure was repeated from the opposite side (steps 5 to 6 in Fig. 2a). In total, 40 specimens were used in this study, whereby for half of the specimens, a one-sided repair (1S), and for the other half, a two-sided repair (2S) was performed. The repair welding was performed by shield metal arc welding (SMAW), illustrated in Fig. 2b. The welding parameters are summarized in Table 3.

After the described repair procedure, HFMI-treatment was performed. For this, two HFMI devices of the manufactures Pitec and HiFIT were used. The same radius of the indenters of 2 mm and a working pressure of 6 bar for both tools was used. According to former investigations [38, 39], the impact frequency of the Pitec-device was adjusted to 90 Hz at the device, and an impact frequency of 270 Hz was estimated using the HiFIT-device. The HFMI-treated welded joints were proofed by visual testing (VT) according to the respective IIW-guideline [22].

Different crack depths a are needed to be available for the two repair cases (1S and 2S). For this reason, the specimens

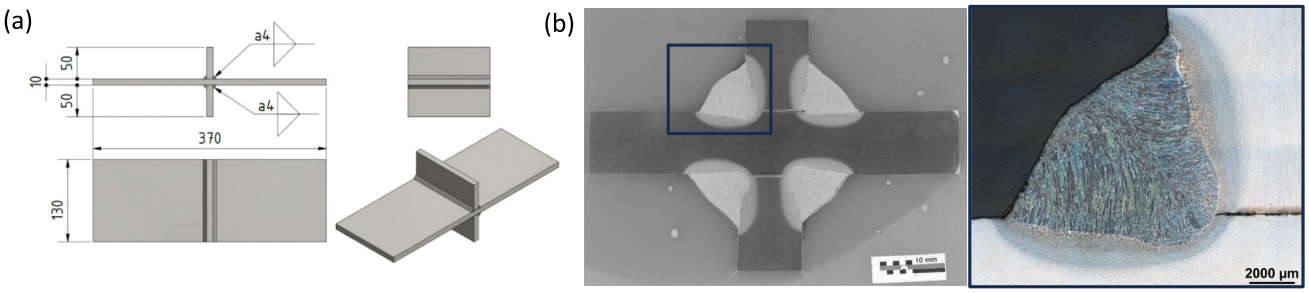

Fig. 1 **a** Specimen dimensions, **b** specimen cross-section, and **c** cross section of single fillet weld

Table 3 Process parameter for initial welding process

	Voltage [V]	Currency [A]	Heat input [kJ/mm]	Welding speed [mm/s]	Efficiency [-]	Wire feed speed [m/min]
Initial GMAW	247	29.4	0.873	6.65	0.8	8.5
Repair (SMAW)	125	95	3.166	3	0.8	-

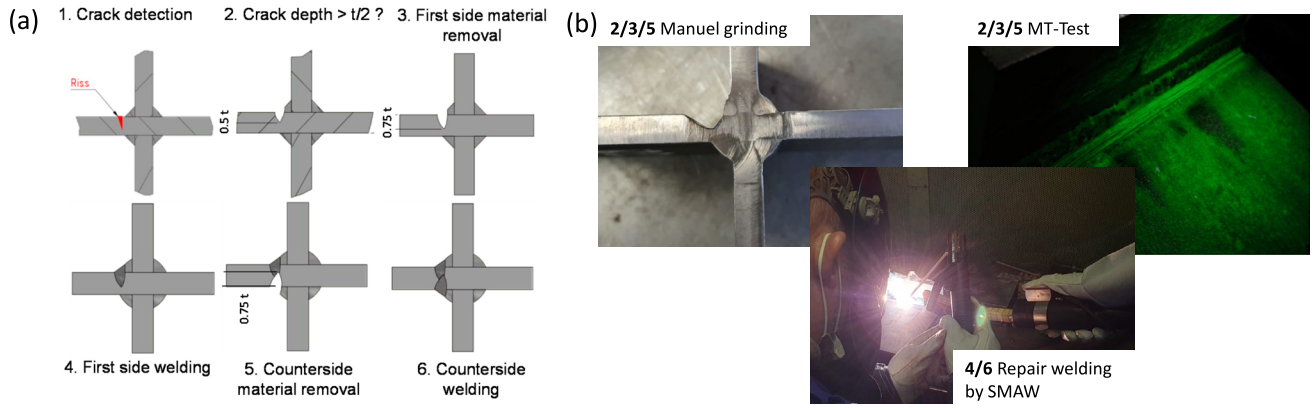

Fig. 2 **a** Principal procedure of the weld repair process [10]. **b** Illustrations of the repair process

were loaded on the resonance-frequency testing machine RUMUL 150 K. A frequency decrease Δf was detected that was caused by propagating cracks associated with a stiffness decrease of the cyclic loaded specimens. A sinusoidal 4-point bending load was applied in this setup. The correlation of $\Delta f \sim a$ from former studies [10] with identical specimens was used. As illustrated in Fig. 5, a shut-down criterion of Δf=0.2 Hz was used for one-sided repair ($a < t/2$), and a shut-down criterion of Δf=1.2 Hz was used for double-sided repairs ($a > t/2$). The test procedure is illustrated in Fig. 3. To assure that only one specific weld toe shows a fatigue failure, the other three weld toes were HFMI-treated for the first test in original condition. After repair-welding, the already treated weld toes were treated again by HFMI to avoid fatigue cracks from other locations than the repair-welded location.

4 Investigation on weld properties

4.1 Geometry

Former studies have shown a clear correlation between local geometrical parameters of welded joints and their fatigue strength [40–42]. Furthermore, based on the results of a previous study [10], an increase of the fatigue strength after repair-welding is attributed to the decrease of stress concentrations at the weld toe. For these reasons, the change of the weld geometry is investigated by means of 2D and 3D scan techniques [43, 44]. The angle of distortion was measured from 2D-scans, illustrated in Fig. 4a. For 3D scanning, the fringe light projection (FLP) sensor micro-epsilon SC3500-120 was used. The weld toe angle according to ISO 5817:2023 [37] was determined from single cross sections taken from 3D scans with a distance of 1 mm, illustrated in Fig. 4a. As seen in Fig. 4b, the angle of distortion β increases by single-sided repair (1S) up to 3.9° (mean). A double-sided weld repair (2S) leads to significant smaller values of β. The weld toe angle α significantly increases after repair (see Fig. 4c). No meaningful difference was determined between 1 and 2S condition. Interestingly, an additional inductive preheated to a temperature of 200 °C that was performed on three specimens leading to even higher values of α. It should be mentioned that the angle of distortion was reported in this study but has no further effect on the fatigue performance because of the application of a four-point bending set-up for fatigue testing, see Section 5.

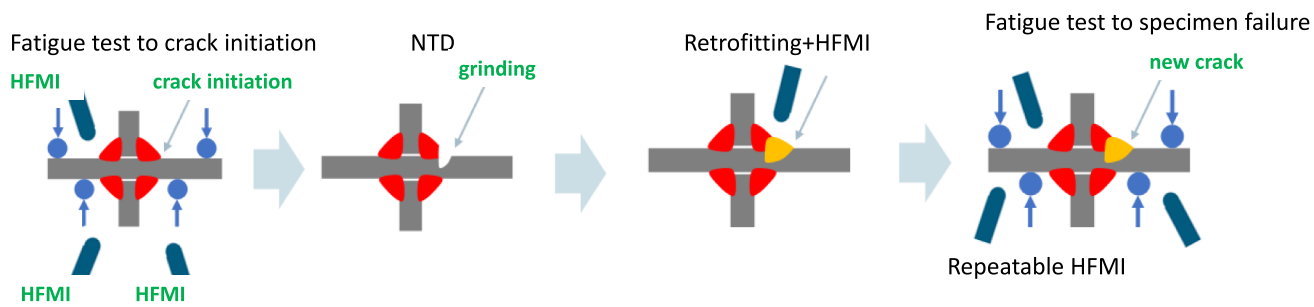

Fig. 3 Illustration of the testing procedure for the investigated specimens

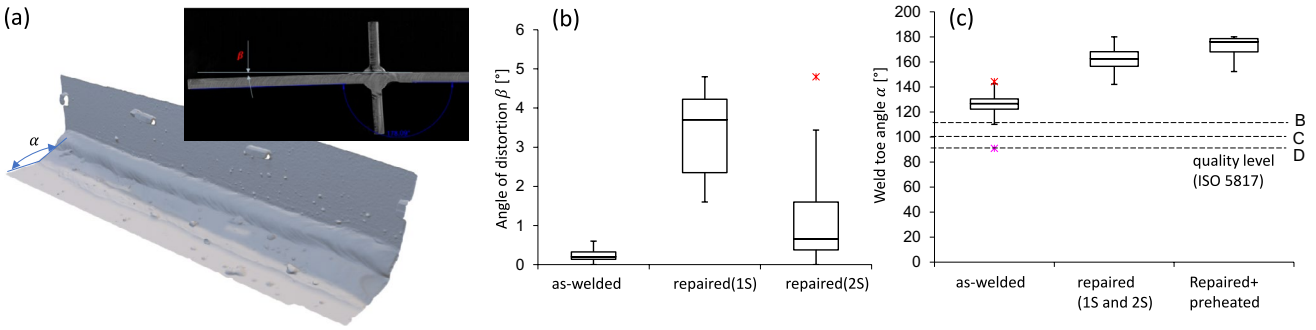

Fig. 4 **a** 3D/2D scan illustration of a specimen in repaired condition and box plots of angle of distortion β (**b**) and weld toe angle α (**c**)

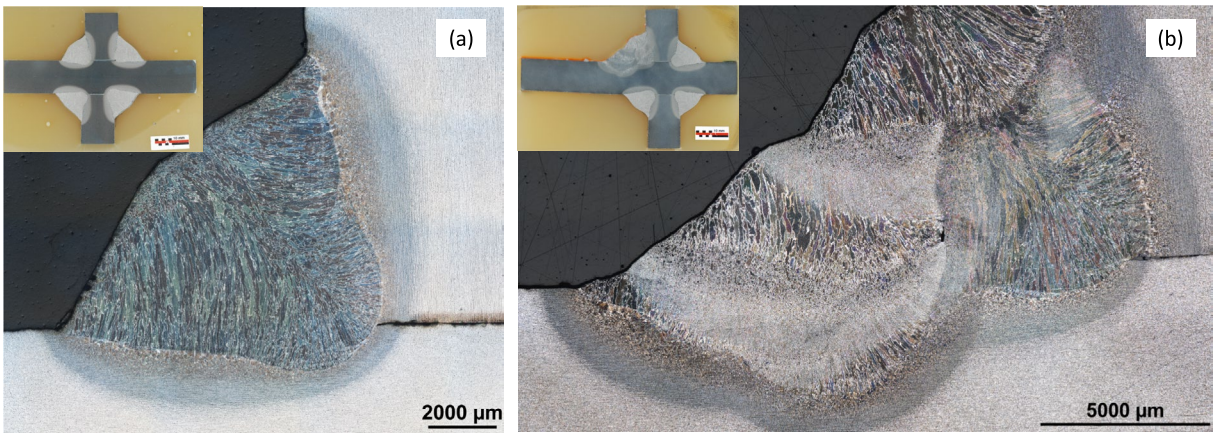

Fig. 5 Cross sections of the specimen in as-welded condition (**a**) and after a single-sided weld repair (1S) (**b**)

4.2 Microstructure and hardness

It is known that the (coarse) grain structure of the heat-affected zone (HAZ) has an influence on the fatigue behavior of welded joints, or more specific, on the fatigue crack propagation rate [45]. For this reason, dimensions and grain structure of the heat-affected zone were investigated (see Fig. 5). Qualitatively, the grain structure of the HAZ in repaired condition is much coarser compared to as-welded condition. Also, the width of the heat-affected zone is as twice bigger compared to as-welded condition. This could be referred to the longer $t_{8/5}$-time of the repair welding process (ca. 13.5 s compared to 4.2 s [10] of the initial welding process).

The toughness of the heat-affected zone (HAZ) is also an important factor to secure that neither a brittle fracture under load nor cold cracks occurs. For that, the maximum hardness values of the HAZ should be 380 HV10 and for some special applications at a maximum of 450HV10 depending on the steel grade and possible heat treatment. These values are also established in the standards DIN EN ISO 15614–1 [46]. Figure 6 displays the cross section and the hardness distribution of the weld details in repaired condition. All hardness measurements were performed according to DIN EN ISO 6507–1:2018–07 [47]. The hardness scale for the measurements was HV1 with an indentation point distance of 0.5 mm. The HAZ of the initial weld shows an average hardness of 295 HV1 compared to repaired condition of 245 HV1. Again, this is referred to the different $t_{8/5}$-time.

4.3 Residual stress state and residual stress relaxation

It is strongly assumed that residual stresses caused by shrinking and phase transformation effects during heating and cooling have a high influence on the fatigue behavior of welded joints. The residual stresses were measured with X-ray diffraction techniques at the {211}-lattice plane with a Ca-Kr-radiation. The collimator diameter for the measurement was 1 mm. The mobile diffractometer Pulstec µ-360 with an 2D-detector (image plate) was used. The stresses in transverse direction were evaluated by the cos α-method [48, 49] assuming an even stress state at the surface layer. Former investigations [50] show quite similar results with

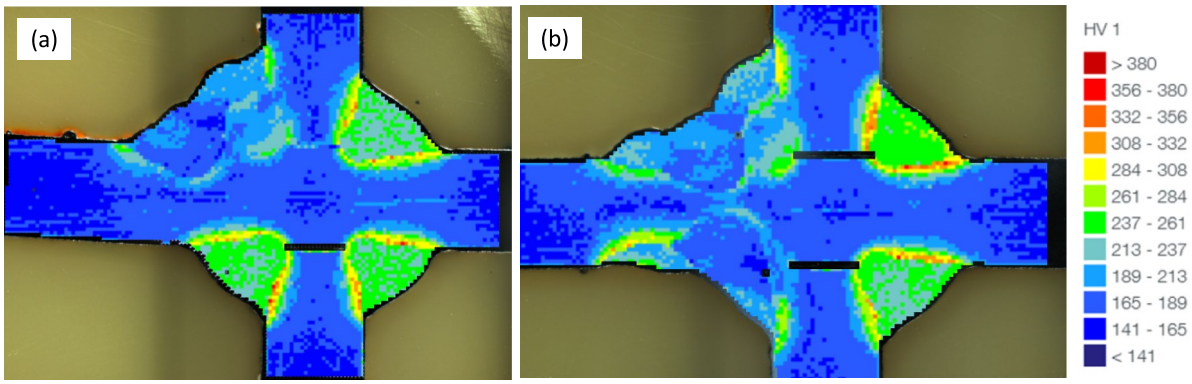

Fig. 6 Micro-hardness mappings of a specimen after single-sided repair (1S) (**a**) and double-sided repair (2S) (**b**)

more commonly used diffractometers with 1D detectors based on the sin ψ^2-method if no coarse grain or texture effects affect the measurements. The measurements were performed within one single line at the specimen starting from the weld bead to the base material.

The residual stress profiles in as-welded (original) condition and after repair-welding are shown in Fig. 7. As can be seen, no high residual stresses in transverse direction could be determined in as-welded condition, like previous investigations showed for similar specimens [10]. After single-sided repair (Fig. 7a), slight tensile residual stresses were determined at the repaired side. On the contrary side, however, high tensile residual stresses up to 300 MPa were determined. Again, after double-sided repair (Fig. 7c), moderate residual stresses were determined.

It is assumed that a high portion of the fatigue life extension by HFMI-treatment is contributed to the presence of compressive residual stresses [22]. Also, the fact whether compressive residual stresses are stable or relax during cyclic loading is important in order understand their effect [51]. Thus, the residual stress state after HFMI-treatment in unloaded condition ($N=0$), after applying one load cycle ($N=1$), and after half of the lifetime ($N=N_f/2$) was determined, summarized in Fig. 8. Also, the full width half maximum (FWHM) is additionally displaced, as a measure of the local hardness of the specimen. If the FWHM changes, cyclic softening or hardening occurs [52]. The compressive residual stresses slightly relax after the first load cycle ($N=0$ to $N=1$). After that, no significant changes during half of the lifetime of the specimens occurs. Both investigated specimens were loaded with a nominal stress range of $\Delta S = 375$ MPa at a stress ratio of $R=0.1$. This leads to a maximum nominal stress of $S_{max} = 416$ MPa in the range of the real yield strength $f_{y,real}$ of the base material. No meaningful change of the FWHM was determined. So, it is assumed that no cyclic softening or hardening occurs at least to half of the lifetime of the specimen.

The transverse residual stresses at the groove center normalized with $f_{y,real}$ is shown in Fig. 9 over the maximum nominal stress S_{max} applied to the specimen and after different numbers of load cycles. As seen in Fig. 9a, no significant residual stress relaxation was determined up to a value of $S_{max} = 0.8\ f_{y,real}$ and up to $S_{max} \approx f_{y,real}$. For the specimen with the highest measured residual stress (PIT, Rep(1 s)), residual stress relaxation after the first load cycle $N=1$ to half of the specimen lifetime was determined (see Fig. 9b). For all other specimens, no meaningful residual stress relaxation was determined to half of the specimen's lifetime.

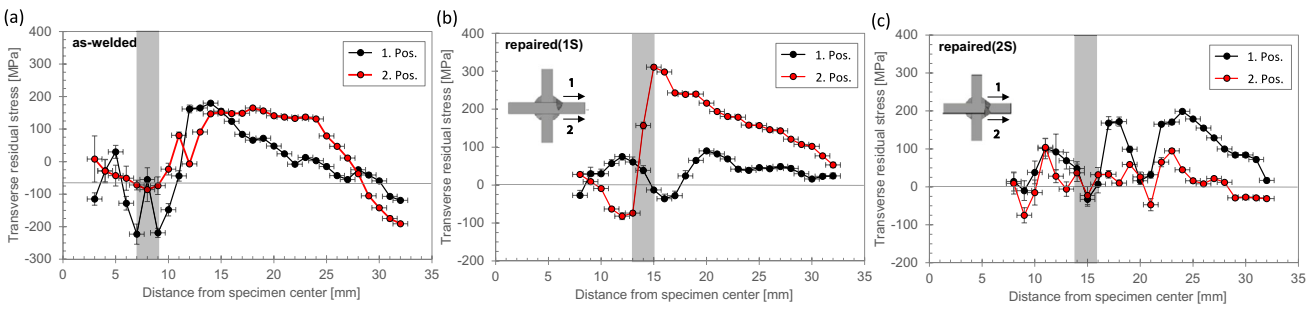

Fig. 7 Residual stress profiles in as-welded condition (**a**), single-sided repair condition (**b**), and double-sided repair condition (**c**)

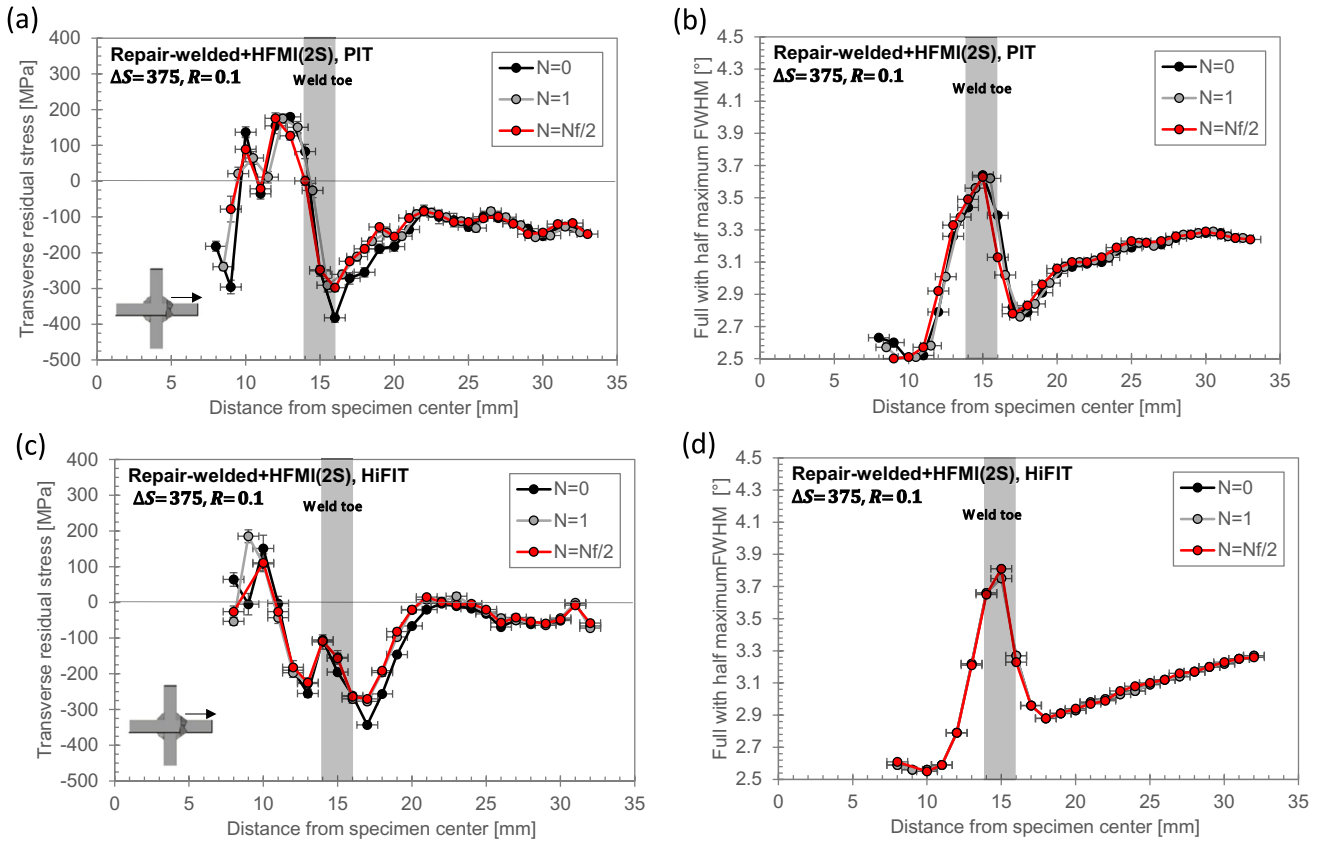

Fig. 8 Residual stress and full width half maximum (FWHM) profiles in double-sided repaired condition after PIT (**a**, **b**) and HiFIT treatment (**c**, **d**)

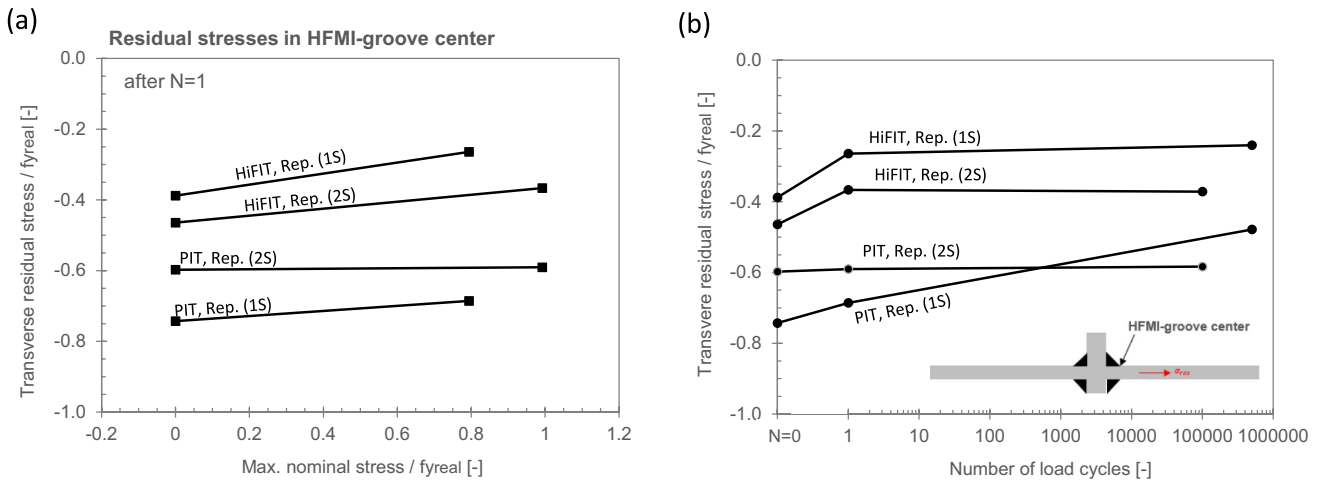

Fig. 9 Normalized transverse residual stress at the groove center of the HFMI-treated specimen in dependency of the maximum nominal stress (**a**) and the number of load cycles (**b**)

5 Fatigue performance

The focus of this work was the comparison of the fatigue performance of the initial-welded specimen and the repaired specimen with and without HFMI-treatment. As an identical stop criterion of the fatigue tests a frequency drop of $\Delta f = 0.2$ Hz was used for the illustrations below and for the evaluation. Note that between a crack depth of $a < t/2$ (one-sided-repair) and $\Delta f = 1.2$ Hz for a crack depth $a > t/2$ (double-sided repair), only slight differences in fatigue life occur. For further information, please refer to former investigations by Schubnell et al. [10], where the differences of fatigue life between the two shut down criteria were investigated in detail. The tests were performed on a servo-hydraulic resonance testing machine RUMUL 150 K with a sinusoidal load and a stress ratio of $R = 0.1$.

The fatigue test results of the specimens in as-welded (original) and repaired condition (single- and double-sided repair) are displayed in Fig. 10. The statistical evaluation was performed according to DIN 50100:2022 [53] in accordance to the IIW-recommendations [54]. The plotted SN-curves correspond to a failure probability P_f of 2.3% and were evaluated with a fixed slope of k=3 according to the IIW-recommendations [54] for joints in as-welded condition. As shown, the specimens in repaired condition reach a similar scatter range in comparison to the specimens in as-welded (original) condition. No significant differences in fatigue life are shown between single-sided (1S) and double-sided (2S) repair.

The fatigue test results of all specimens and corresponding SN-curves are displayed in Fig. 11. The horizontal line corresponds to the maximum nominal stress $S_{max} = \Delta S/(1\text{-}R)$ limit according to several recommendations and the real yield strength of the base material $f_{y,real}$ (see Table 2). In the case of repaired and HFMI-treated specimens, several failure cases occurred during fatigue testing, illustrated in Fig. 12. Nearly half of the tested specimens showed a fatigue failure in a distance of 5 to 10 mm in front of the weld toe (referred as base material failure) or show mixed-mode failure (cracks are visible at the base material and at the weld toe at the same time). However, all the specimens that showed these failure cases are still used for statistical evaluation under the assumption that the weld toe would fail after a small number of additional load cycles. Also, several runouts ($N > 10^7$ load cycles) were observed at load levels where other specimens showed a comparable early fatigue failure but are not included in the statistical evaluation. As shown in Fig. 11, a high scatter was determined for the repaired and HFMI-treated specimens. The load levels that are needed in order to observe a failure of the specimens are significantly above the IIW-recommendations [22] and the DASt guideline 026 [23].

The statistical evaluation of all fatigue tests is shown in Table 4 based on the fatigue test data given in Table 5. The evaluation was performed with a variable slope (k=var.) and a fixed slope (k=fix.) according to the guidelines [22, 54]. The statistical evaluation includes all failure cases seen in Fig. 12. The pragmatic reason is that not enough specimens were available for a sufficient number of tests, and in this way, a conservative statistical evaluation could be performed. As measure of the scatter of the fatigue tests results the scatter range $T_S = \Delta S_{97,7\%}/ = \Delta S_{2,3\%}$ was calculated. As shown, all the fatigue test series in repaired condition exceed the typical scatter range to $T_S \approx 1.5$ according to Haibach

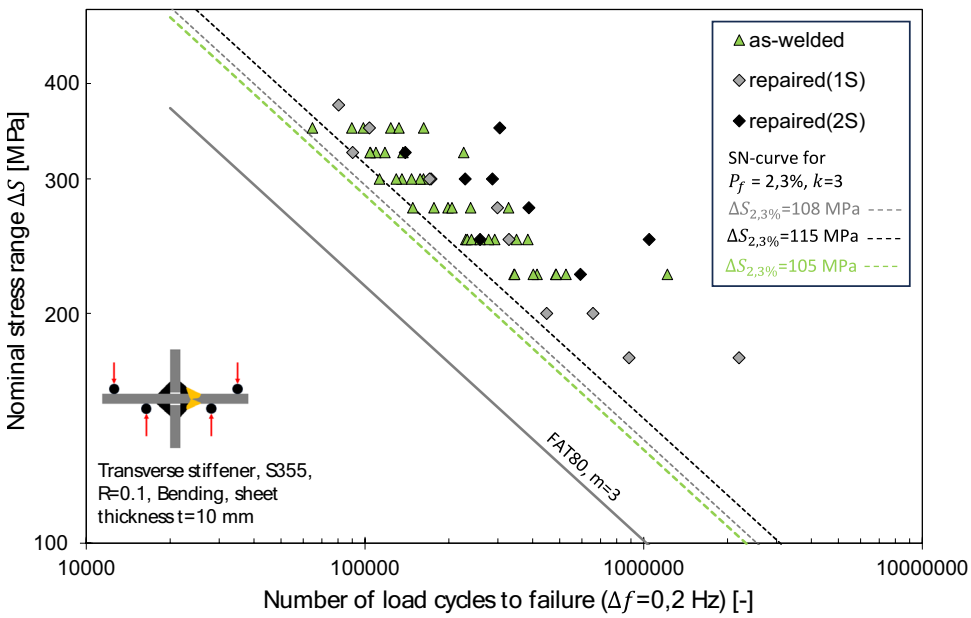

Fig. 10 SN curve for specimens without HFMI-treatment

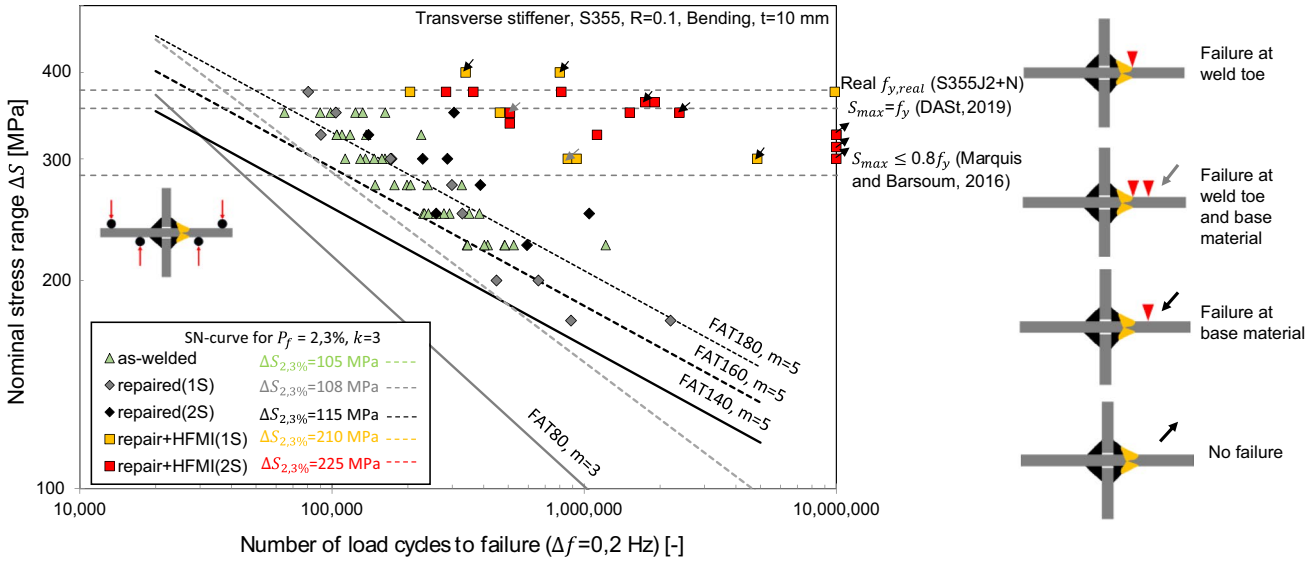

Fig. 11 SN curve for specimens with and without HFMI-treatment with the corresponding limits of the maximum nominal stresses according to Marquis and Barsoum [22] and the German DASt-guideline 026 [23] as well as the real yield strength of the base material $f_{y,\mathrm{real}}$ (415 MPa)

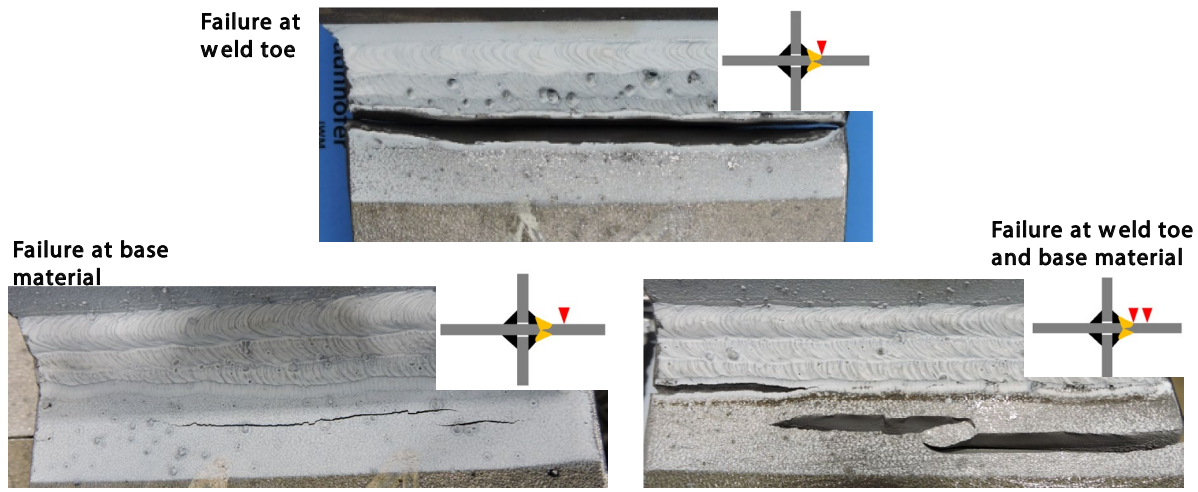

Fig. 12 SN-curve for specimens with and without HFMI-treatment with the corresponding limits of the maximum nominal stresses according to Marquis and Barsoum [22] and the German DASt guideline 026 [23] as well as the real yield strength of the base material $f_{y,\mathrm{real}}$ (415 MPa)

[55]. For a better comparison with the corresponding FAT-classes according to the IIW guidelines [54], a factor of 0.8 according to Radaj [56] for the comparison of fatigue strength in bending and tension was used. Also, a correction according to the give enhancement factors $f(R) = -0.4\ R + 1.2$ according to Hobbacher [54] was used for the $R = 0.1$ under the assumption that no high residual stresses are present (residual stress bellow 0.2 f_y). The residual stress measurements show that this is the case at the weld toe (Pos.1). The comparison of the corrected $\Delta S_{2,3\%}$ shows similar values compared to the corresponding FAT-classes of transverse stiffeners of FAT 80 without HFMI-treatment. In repaired and HFMI-treated condition, the values of $\Delta S_{2,3\%}$ are still above the corresponding FAT-class of 140.

6 Conclusions

In this work, the fatigue strength of repair-welded and HFMI-treated specimens were quantified. Regarding the high retrofit demand of welded structures in bridges, the combination of repair welding and mechanical post weld

Table 4 Statistical evaluation of fatigue test data and comparison with guidelines

Condition	Evolution k=var			Evolution k=fix		*Tension	**$R \geq 0.5$	Recommendation	
Parameter	$\Delta S_{2,3\%}$ [MPa]	k[-]	T_S[-]	$\Delta S_{2,3\%}$[MPa]	k[-]	$\Delta S_{2,3\%}$[MPa]	$\Delta S_{2,3\%}$[MPa]	FAT	Ref
AW	126	3.61	1.38	105	3	84	91	80	[54]
Repaired(1S)	128	3.59	1.34	108	3	86	93	80	[54]
Repaired(2S)	104	2.68	2.68	115	3	92	99	80	[54]
Repaired(1S) + HFMI	208	4.89	1.68	210	5	168	-	140	[22]
Repaired(2S) + HFMI	217	4.45	1.72	226	5	183	-	140	[22]

Scatter range $T_S = \Delta S_{97,7\%} / = \Delta S_{2,3\%}$ (correspond to failure probability of P_f of 97.7% and 2.3%)

*Ratio of fatigue test results in tension and bending ≈ 0.8 according to Radaj [56], verified by comparison between Schubnell et. al. [10] and Gkatzogiannis et. al. [39]

**Stress ration $f(R) = -0.4R + 1.2$ according to Hobbacher (2016) [54]

treatment by HFMI is an excellent possibility to increase the fatigue strength of the retrofitted weld detail and avoids further repair measures in the future. The same retrofitting approach (repair welding) than in previous studies by Ladendorf et al. [1] and Schubnell et al. [10] was used. In contrary, SMAW is used in this study as repair welding process. Different conditions of transverse stiffeners were investigated: single-sided (1S) and double-sided (2S) repair welding depending on the crack depth and 1S/2S repair combined with HFMI-treatment (1S + HFMI, 2S + HFMI). Additionally, residual stress state and residual stress relaxation, as well as the geometrical parameter weld toe angle α and the angle of distortion β, microstructure, and hardness, were determined. The following conclusions were made:

- The specimens in repaired condition show higher weld toe angles (median 163°), compared to the original condition (median 126°) but higher angles of distortion (0.2 median in original/as-welded condition and 3.7° in (1S) and 0.65° in (2S) repair-welded condition).
- The fatigue life of the investigated specimens in repaired condition is (for both conditions 1S and 2S) in the similar range than in the original condition. The fatigue strength of the original welded detail could be restored in this study by manual SMAW.
- A significant extension of fatigue strength (> 60%) was reached by the combination of repair-welding and HFMI-treatment compared to the repair-welded condition without any further post weld treatment.
- A low level of residual stress relaxation under cyclic loading was determined for the HFMI-treated specimen even if high nominal stresses S_{max} up to 80% and 100% of the real materials yield strength $f_{y,real}$ are applied. The authors assume that this is related to applied bending load and the level of residual stress relaxation may be higher under tension loading.
- The applied load levels for repaired and HFMI-treated specimens exceed the recommendation regarding S_{max} of $S_{max} \leq f_y$ [23] or $S_{max} \leq 0.8 f_y$ [22] (with f_y=355 MPa); however, for low load levels ($S_{max} > 0.8 f_y$), no failure of the specimen could be reached until reaching 10^7 load cycles. Again, it is assumed that the bending load is responsible for this issue.
- Assuming a ratio of 0.8 regarding the fatigue strength of welded joints under tensional and bending loads, the determined fatigue strength of specimens without post weld treatment (as-welded/original and repaired condition), and the determined fatigue strength was close to the corresponding fatigue class FAT80 [54]. For the HFMI-treated condition, higher values compared to the corresponding fatigue class of FAT140 [22, 23] were determined.

This study shows significant potential of HFMI-treatment in combination with repair-welding for the retrofitting of welded structures. Next step of the current research is the application of the process to large-scale components in order to address more realistic conditions of real retrofit cases in welded structures.

Table 5 Fatigue test data

Before repair			After repair				
ΔS[MPa]	$N(\Delta f$=0.2 Hz) [-]	$N(\Delta f$=1.2 Hz) [-]	ΔS[MPa]	$N(\Delta f$=0.2 Hz) [-]	$N(\Delta f$=1.2 Hz) [-]	β[°]	Condition
350	123,800	-	200	448,800	698,800	1.9	Repaired(1S)
350	162,400	-	175	2,201,200	3,351,900	2.5	Repaired(1S)
350	64,800	-	200	657,900	849,100	2.6	Repaired(1S)
325	104,700	-	300	172,500	230,000	2.4	Repaired(1S)
325	136,800	-	275	298,700	393,700	1.6	Repaired(1S)
325	109,500	-	225	324,300	456,600	1.8	Repaired(1S)
300	135,800	-	350	103,700	134,800	4.8	Repaired(1S)
300	162,200	-	250	328,700	452,600	4.3	Repaired(1S)
300	129,600	-	325	90,400	138,000	4.3	Repaired(1S)
275	327,400	-	375	80,500	110,900	3.8	Repaired(1S)
275	198,500	-	300	170,700	226,800	3.6	Repaired(1S)
275	176,800	-	175	886,700	1,162,000	4.7	Repaired(1S)
250	292,100	-	250	1,047,500	1,244,400	−1.6	Repaired(2S)
250	230,200	-	350	304,600	387,500	−2.5	Repaired(2S)
250	233,000	-	275	387,600	500,100	−0.3	Repaired(2S)
250	350,100	-	325	139,600	183,600	0	Repaired(2S)
225	1,216,800	-	300	286,900	372,700	0.7	Repaired(2S)
225	342,700	-	225	593,500	778,300	−1.3	Repaired(2S)
225	483,300	-	300	228,900	312,700	−0.6	Repaired(2S)
350	414,800	-	400	800,000	890,700	1.6	Repaired(1S) + HFMI
225	98,700	140,600	400	338,700	376,500	2.2	Repaired(1S) + HFMI
350	132,400	169,000	350	463,100	520,700	3.6	Repaired(1S) + HFMI
350	89,700	119,500	300	4,851,700	4,940,400	4.1	Repaired(1S) + HFMI
350	226,000	281,300	300	861,300	1,003,800	4.4	Repaired(1S) + HFMI
325	118,000	158,400	375	203,900	259,500	4.1	Repaired(1S) + HFMI
325	104,400	148,200	300	932,300	107,4400	4.2	Repaired(1S) + HFMI
325	157,900	197,500	375	9,860,900	9,963,300	4	Repaired(1S) + HFMI
300	146,900	205,700	225	593,500	778,300	−1.3	Repaired(2S) + HFMI
300	112,800	164,900	350	508,000	645,400	0.6	Repaired(2S) + HFMI
300	148,400	203,100	362.5	1,748,700	1,949,100	−0.3	Repaired(2S) + HFMI
275	205,100	290,000	362.5	1,904,200	2,067,500	0.9	Repaired(2S) + HFMI
275	239,500	329,400	350	2,388,000	2,640,500	0.3	Repaired(2S) + HFMI
275	241,200	344,300	375	363,300	433,500	1.6	Repaired(2S) + HFMI
250	384,400	509,700	325	1,124,300	1,277,900	2.2	Repaired(2S) + HFMI
250	277,900	376,800	350	1,518,000	1,741,000	−0.8	Repaired(2S) + HFMI
250	258,900	344,300	375	812,300	915,100	0.5	Repaired(2S) + HFMI
225	344,700	452,000	337.5	507,000	613,700	−0.4	Repaired(2S) + HFMI
225	485,000	650,100	375	283,200	350,400	0.1	Repaired(2S) + HFMI
225	526,100	686,900	312.5	10,000,000	-	−4.8	Repaired(2S) + HFMI
225	402,100	540,500	325	10,000,000	-	−1	Repaired(2S) + HFMI
350	94,600	128,600	300	10,000,000	-	−1.6	Repaired(2S) + HFMI

Funding Open Access funding enabled and organized by Projekt DEAL. This work was funded by the German Federal Ministry of Economic Affairs and Climate Action (BMWK) (Award Number: IGF No. 22.566 N).

Declarations

Competing interests The authors declare no competing interests.

References

1. Ladendorf P, Knödel P, Ummenhofer T, Schubnell J, Farajian M (2019) „Retrofit Engineering": Entwickeln und Validieren einer Prozedur zur schweißtechnischen Instandsetzung von Großbauteilen. Congress of the German Welding Society (DVS), Roststock Germany
2. German Federal Ministry of Transport (2006) Bericht über die Qualität, Dauerhaftigkeit und Sicherheit von Spannbetonbrücken, Bau und Stadtentwicklung des Deutschen Bundestages (in German). http://www.bmvi.de/. Berlin
3. Dexter RJ, Ocel JM (2013) Manual for repair and retrofit of fatigue cracks in steel bridges, Report No. FHWA-IF-13–020, 2nd edn. University of Minnesota
4. Yokoyama K, Miki C (2017) Participatory database of repair cases on fatigue damaged welded structures. Int J Fatigue 101:385–396. https://doi.org/10.1016/J.IJFATIGUE.2017.01.010
5. Miki C (2010) Retrofi tting engineering for fatigue damaged steel structures. IIW-Document IIW-XIII-2284r1–09
6. Miki C, Hanji T, Tokunaga K (2012) Weld repair for fatigue-cracked joints in steel bridges by applying low temperature transformation welding wire. Weld World 56(3–4):40–50. https://doi.org/10.1007/BF03321334
7. Cruz PJS, Frangopol DM, Neves LC (2006) Bridge maintenance, safety, management, life-cycle performance and cost. In: Proceedings of the 3rd international conference on bridge maintenance, safety and management
8. Chen Z, Liu Y, Qian H, Wang P, Liu Y (2023) Effect of repair welding on the fatigue behavior of AA6082-T6 T-joints in marine structures based on FFS and experiments. Ocean Eng 281:114676. https://doi.org/10.1016/J.OCEANENG.2023.114676
9. Seo JW, Kwon SJ, Lee CW, Lee DH, Goo BC (2021) Fatigue strength and residual stress evaluation of repair welding of bogie frame for railway vehicles. Eng Fail Anal 119:104980. https://doi.org/10.1016/J.ENGFAILANAL.2020.104980
10. Schubnell J, Ladendorf P, Sarmast A, Farajian M, Knödel P (2021) Fatigue performance of high-and low-strength repaired welded steel joints. Metals (Basel) 11(2):293. https://doi.org/10.3390/met11020293
11. Yu B, Chen Z, Wang P, Song X (2023) A comparative study on the mechanical behavior of S355J2 steel repair-welded joints. J Constr Steel Res 205:107878. https://doi.org/10.1016/J.JCSR.2023.107878
12. Al-Salih H, Bennett C, Matamoros A, Collins W, Li J (2020) Repairing distortion-induced fatigue in steel bridges using a CFRP-steel retrofit. In: Structures Congress 2020 - Selected Papers from the Structures Congress 2020, pp 273–284 https://doi.org/10.1061/9780784482896.026
13. Siwowski T, Kulpa M, Janas L (2019) Remaining fatigue life prediction of welded details in an orthotropic steel bridge deck. J Bridg Eng 24(12):05019013. https://doi.org/10.1061/(asce)be.1943-5592.0001490
14. Alencar G, de Jesus A, da Silva JGS, Calçada R (2019) Fatigue cracking of welded railway bridges: a review. Eng Fail Anal 104:154–176. https://doi.org/10.1016/j.engfailanal.2019.05.037. Elsevier Ltd
15. Teixeira de Freitas S, Kolstein H, Bijlaard F (2017) Fatigue assessment of full-scale retrofitted orthotropic bridge decks. J Bridg Eng 22(11):04017092. https://doi.org/10.1061/(asce)be.1943-5592.0001115
16. Yu QQ, Wu YF (2018) Fatigue retrofitting of cracked steel beams with CFRP laminates. Compos Struct 192:232–244. https://doi.org/10.1016/j.compstruct.2018.02.090
17. Walbridge S, Liu Y (2018) Fatigue design, assessment, and retrofit of bridges. J Bridg Eng 23(12):02018001. https://doi.org/10.1061/(asce)be.1943-5592.0001314
18. Zhao P, Yu B, Wang P, Liu Y, Song X (2023) Influence of repair welding on the fatigue behavior of S355J2 T-Joints. Materials 16(10):3682. https://doi.org/10.3390/MA16103682
19. Ahola A, Lipiäinen K, Lindroos J, Koskimäki M, Laukia K, Björk T (2023) On the fatigue strength of welded high-strength steel joints in the as-welded, post-weld-treated and repaired conditions in a typical ship structural detail. J Mar Sci Eng 11(3):644. https://doi.org/10.3390/JMSE11030644
20. Miki C, Konishi T (2007) Retrofit engineering for steel bridge structures in Japan. IABSE Symposium: Improving Infrastructure Worldwide, pp 14–19. https://doi.org/10.2749/222137807796119555
21. Miki C, Takenouchi H, Mori T, Ohkawa S (1989) Repair of fatigue damage in cross bracing connections in steel girder bridges. Doboku Gakkai Ronbunshu 1989(404):53–61. https://doi.org/10.2208/jscej.1989.404_53
22. Marquis GB, Barsoum Z (2016) IIW recommendation for the HFMI treatment for improving the fatigue strength of welded joints. Springer, Singapore
23. DASt (2019) DASt-Richtlinie 026, Ermüdungsbemessung bei Anwendung höherfrequenter Hämmerverfahren. Stahlbau Verlags- und Service GmbH
24. Tominaga T, Matsuoka K, Sato Y, Suzuki T (2008) "Fatigue improvement of weld repaired crane runway girder by ultrasonic impact treatment, Doc. IIW-1860 Weld World 52(11/12):50–62. https://doi.org/10.1007/bf03266682
25. Maddox SJ, Doré MJ, Smith SD (2011) A case study of the use of ultrasonic peening for upgrading a welded steel structure. Weld World 55(9–10):56–67. https://doi.org/10.1007/BF03321321/METRICS
26. Zhang H, Wang D, Xia L, Lei Z, Li Y (2015) Effects of ultrasonic impact treatment on pre-fatigue loaded high-strength steel welded joints. Int J Fatigue 80:278–287. https://doi.org/10.1016/J.IJFATIGUE.2015.06.017
27. Kudryavtsev Y et al (2007) Rehabilitation and repair of welded elements and structures by ultrasonic peening. Weld World 51(7–8):47–53. https://doi.org/10.1007/BF03266585
28. Al-Karawi H, von Bock und Polach RUF, Al-Emrani M (2020) Fatigue crack repair in welded structures via tungsten inert gas remelting and high frequency mechanical impact. J Constr Steel Res 172:106200. https://doi.org/10.1016/J.JCSR.2020.106200
29. Al-Karawi H, von Bock und Polach RUF, Al-Emrani M (2021) Fatigue life extension of existing welded structures via high frequency mechanical impact (HFMI) treatment. Eng Struct 239:112234. https://doi.org/10.1016/J.ENGSTRUCT.2021.112234
30. Leitner M, Barsoum Z, Schäfers F (2016) Crack propagation analysis and rehabilitation by HFMI of pre-fatigued welded structures. Weld World 60(3):581–592. https://doi.org/10.1007/s40194-016-0316-x

31. Branco CM, Infante V, Baptista R (2004) Fatigue behaviour of welded joints with cracks, repaired by hammer peening. Fatigue Fract Eng Mater Struct 27(9):785–798. https://doi.org/10.1111/J.1460-2695.2004.00777.X
32. Fueki R, Takahashi K (2018) Prediction of fatigue limit improvement in needle peened welded joints containing crack-like defects. Int J Struct Integr 9(1):50–64. https://doi.org/10.1108/IJSI-03-2017-0019/FULL/PDF
33. Fueki R, Takahashi K, Houjou K (2015) Fatigue limit prediction and estimation for the crack size rendered harmless by peening for welded joint containing a surface crack. Mater Sci Appl 06(06):500–510. https://doi.org/10.4236/MSA.2015.66053
34. Houjou K, Takahashi K, Ando K, Abe H (2014) Effect of peening on the fatigue limit of welded structural steel with surface crack, and rendering the crack harmless. Int J Struct Integr 5(4):279–289. https://doi.org/10.1108/IJSI-12-2013-0048/FULL/PDF
35. Ummenhofer T et al (2011) Abschlussbericht Forschungsprogramm REFRESH, Lebensdauerverlängerung bestehender und neuer geschweißter Stahlkonstruktionen. FOSTA – Research Association for Steel Application Association in Germany, Düsseldorf
36. DIN EN 10025–2:2019–10 (2019) Warmgewalzte Erzeugnisse aus Baustählen - Teil 2: Technische Lieferbedingungen für unlegierte Baustähle
37. DIN Deutsches Institut für Normung e.V. (2023) Deutsche Fassung EN ISO 5817:2023: Schweißen – Schmelzschweißverbindungen an Stahl, Nickel, Titan und deren Legierungen (ohne Strahlschweißen) – Bewertungsgruppen von Unregelmäßigkeiten
38. Schubnell J, Pontner P, Wimpory RC, Farajian M, Schulze V (2020) The influence of work hardening and residual stresses on the fatigue behavior of high frequency mechanical impact treated surface layers. Int J Fatigue 134:125–138. https://doi.org/10.1016/j.ijfatigue.2019.105450
39. Gkatzogiannis S, Schubnell J, Knoedel P, Farajian M, Ummenhofer T, Luke M (2021) Investigating the fatigue behaviour of small scale and real size HFMI-treated components of high strength steels. Eng Fail Anal 123:105300. https://doi.org/10.1016/J.ENGFAILANAL.2021.105300
40. Barsoum Z, Jonsson B (2007) Fatigue assessment and LEFM analysis of cruciform joints fabricated with different welding processes. Weld World 52(7–8):93–105. https://doi.org/10.1007/BF03266657
41. Jonsson B, Samuelsson J, Marquis GB (2011) Development of weld quality criteria based on fatigue performance. Weld World 55(11–12):79–88. https://doi.org/10.1007/BF03321545
42. Nykänen T, Marquis GB, Björk T (2009) A simplified fatigue assessment method for high quality welded cruciform joints. Int J Fatigue 31(1):79–87
43. Schubnell J et al (2020) Influence of the optical measurement technique and evaluation approach on the determination of local weld geometry parameters for different weld types. Weld World 64(2):301–316. https://doi.org/10.1007/s40194-019-00830-0
44. Renken F et al (2021) An algorithm for statistical evaluation of weld toe geometries using laser triangulation. Int J Fatigue 149:106293. https://doi.org/10.1016/J.IJFATIGUE.2021.106293
45. Fricke W (2014) Recent developments and future challenges in fatigue strength assessment of welded joints. Proc Inst Mech Eng C J Mech Eng Sci 229:1224–1239. https://doi.org/10.1177/0954406214550015
46. DIN EN ISO 15614–1:2017–12 (2017) Anforderung und Qualifizierung von Schweißverfahren für metallische Werkstoffe - Schweißverfahrensprüfung - Teil 1: Lichtbogen- und Gasschweißen von Stählen und Lichtbogenschweißen von Nickel und Nickellegierungen (ISO 15614–1)
47. DIN EN ISO 6507–1:2018–07 (2018) Metallic materials - Vickers hardness test - part 1: test method. Beuth Verlag
48. Taira S, Tanaka K, Yamasaki T (1978) A method of X-ray microbeam measurement of local stress an its application to fatigue crack growth problems. J Soc Mater Sci 27(294):251–256
49. Tanaka K (2019) The cosα method for X-ray residual stress measurement using two-dimensional detector. Mech Eng Rev 6(1):18-00378-18–00378. https://doi.org/10.1299/mer.18-00378
50. Sarmast A, Schubnell J, Carl E, Hinterstein J-M, Preußner J (2023) Residual stress analysis in industrial parts: a comprehensive comparison of XRD methods. J Mater Sci Submitted(X):X
51. Schubnell J et al (2020) Residual stress relaxation in HFMI-treated fillet welds after single overload peaks. Weld World 64(6):1107–1117. https://doi.org/10.1007/S40194-020-00902-6/FIGURES/9
52. Wang Y, Tomota Y, Harjo S, Gong W, Ohmura T (2016) In-situ neutron diffraction during tension-compression cyclic deformation of a pearlite steel. Mater Sci Eng A 676:522–530. https://doi.org/10.1016/J.MSEA.2016.08.122
53. (2022) DIN 50100–2022–12: Schwingfestigkeitsversuch – Durchführung und Auswertung von zyklischen Versuchen mit konstanter Lastamplitude für metallische Werkstoffproben und Bauteile (in German) Beuth Verlag, Berlin
54. Hobbacher AF (2016) Recommendations for fatigue design of welded joints and components, 2th illust. Springer
55. Haibach E (2006) Betriebsfestigkeit: Verfahren und Daten zur Bauteilberechnung (in German), 3rd edn. Springer, Wiesbaden
56. Radaj D, Vormwald M (2007) Ermüdungsfestigkeit (in German), Grundlagen für Ingenieure, 3te, neube ed. Springer Berlin Heidelberg New York